Inorganic Chemistry

Article

pubs.acs.org/IC

Accurate Rate Constants for Decomposition of Aqueous Nitrous Acid

Mark S. Rayson, John C. Mackie, Eric M. Kennedy, and Bogdan Z. Dlugogorski*

Process Safety and Environment Protection Research Group, School of Engineering, The University of Newcastle, Callaghan, New South Wales 2308, Australia

Supporting Information

ABSTRACT: Decomposition of nitrous acid in aqueous solution has been studied by stopped flow spectrophotometry to resolve discrepancies in literature values for the rate constants of the decomposition reactions. Under the conditions employed, the rate-limiting reaction step comprises the hydrolysis of NO_2. A simplified rate law based on the known elementary reaction mechanism provides an excellent fit to the experimental data. The rate constant, 1.34×10^{-6} M^{-1} s^{-1}, is thought to be of higher accuracy than those in the literature as it does not depend on the rate of parallel reaction pathways or on the rate of interphase mass transfer of gaseous reaction products. The activation energy for the simplified rate law was established to be 107 kJ mol^{-1}. Quantum chemistry calculations indicate that the majority of the large activation energy results from the endothermic nature of the equilibrium $2HNO_2 \leftrightarrows NO + NO_2 + H_2O$. The rate constant for the reaction between nitrate ions and nitrous acid, which inhibits HNO_2 decomposition, was also determined.

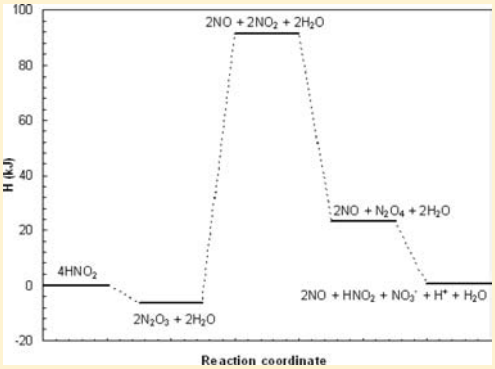

INTRODUCTION

Motivation for the study of nitrous acid decomposition is diverse, with the reactions playing important roles in many industrial and environmental processes. Industrially, decomposition of nitrous acid is a significant process occurring in the manufacture of nitric acid, wherein a gaseous NO_x stream is absorbed in water,[1,2] and in synthesis reactions involving nitrous acid (i.e., nitrosation reactions) where the NO_x side products pose a toxicity hazard.[3,4] In atmospheric chemistry, reactions of nitrous acid and NO_x have received attention owing to their importance in acid deposition on the earth's surface and their role in smog formation,[5] while the reactions may be of biological importance under certain conditions where nitrous acid decomposition could contribute to NO production in the body.[6] Decomposition of nitrous acid can be employed as a source of NO in the laboratory[7] and has been implicated in the release of nitrogen oxides from plants.[8] Because of these considerations, the kinetics of nitrous acid decomposition have received considerable attention in the literature; however, the reported rate constants exhibit significant disagreement.

The present study aims to establish accurate rate constants for decomposition of nitrous acid to enable kinetic modeling of NO_x formation that results as a side reaction during nitrosation reactions, in particular, sensitization of emulsion blasting agents via ammonia nitrosation. Nitrosation of ammonia (reaction 1) aims to produce small nitrogen bubbles within the explosive which act as hot spots to propagate the explosion front through the bulk explosive and result in more reliable and efficient detonation.[9] Formation of NO_x as a side product of ammonia nitrosation, however, poses a hazard to miners prior to explosive detonation, particularly in confined underground mines. For industrial applications such as this, accurate knowledge of the kinetics of the decomposition of nitrous acid is essential to safely implementing nitrosation reactions

$$HNO_2 + NH_3 \rightarrow N_2 + 2H_2O \quad (1)$$

The reaction kinetics of the decomposition of nitrous acid were first elucidated by Abel and Schmidt,[10] who discovered a rate law fourth order in nitrous acid concentration and inversely proportional to the square of the NO partial pressure (i.e., NO concentration), in a well-mixed gas−liquid reactor. Assuming that dissolved NO was in equilibrium with the gas phase in accordance with Henry's law, the kinetics follow eq 2. The reaction was demonstrated to have a stoichiometry of three moles of nitrous acid decomposing to produce two moles of NO and one mole of nitric acid (reaction 3).

$$-\frac{d[HNO_2]}{dt} = \frac{k_{fwd}[HNO_2]^4}{[NO]^2} \quad (2)$$

$$3HNO_2 \rightarrow 2NO + NO_3^- + H^+ + H_2O \quad (3)$$

Equation 2 can be rationalized by assuming that an equilibrium establishes rapidly between nitrous acid, dissolved NO, and NO_2 (reaction 4) and that hydrolysis of NO_2 (reaction 5) comprises the rate-limiting reaction step. Hydrolysis of NO_2 consists of a reaction second order in NO_2 concentration, while two moles of nitrous acid are required to produce one mole each of NO and NO_2. This yields an overall rate law fourth order in HNO_2 concentration and gives $k_{fwd} = 3K_4^2k_5$. Combining reactions 4 and 5 yields the stoichiometry identified in reaction 3. Derivations are

Received: September 23, 2011
Published: February 3, 2012

   dx.doi.org/10.1021/ic202081z | Inorg. Chem. 2012, 51, 2178−2185

provided in the Supporting Information.

$$2HNO_2 \leftrightarrows NO + NO_2 + H_2O,\ k_4,\ k_{-4} \quad (4)$$

$$2NO_2 + H_2O \rightarrow HNO_2 + NO_3^- + H^+,\ k_5 \quad (5)$$

Reactions 4 and 5 proceed via N_2O_3 and N_2O_4 intermediates, respectively, which typically exist in equilibrium with NO and NO_2. Reactions 6–9 below describe the commonly accepted elementary mechanism[11,12]

$$2HNO_2 \leftrightarrows N_2O_3 + H_2O \quad (6)$$

$$N_2O_3 \leftrightarrows NO + NO_2 \quad (7)$$

$$2NO_2 \leftrightarrows N_2O_4 \quad (8)$$

$$N_2O_4 + H_2O \leftrightarrows HNO_2 + NO_3^- + H^+ \quad (9)$$

Schwartz and White[12] performed a comprehensive review of experimental studies related to the absorption of NO and NO_2 in water. Part of that study reviewed the decomposition of nitrous acid, which constitutes the reverse process of NO_x dissolution. The review by Schwartz and White recommended a set of values for the rate and equilibrium constants of 4 and 5 based on a consensus of literature values, taken from studies employing a variety of methods including gas absorption, isotope exchange, flash photolysis, pulse radiolysis, and UV–vis spectrophotometry. The rate constants determined using different methods vary greatly, resulting in considerable uncertainty in the suggested values for the rate constants. The majority of studies reviewed were concerned with either reaction 4 or 5 (or their component reactions such as reactions 7 and 8) occurring in isolation. For example, the value of k_6 comes from the isotope exchange experiments of Bunton and Stedman[13] and the diazotization experiments of Hughes and Ridd,[14] while the value of k_9 was recommended based on a consensus of rate constants from studies concerned with the dissolution of gaseous NO_2/N_2O_4 in water and the pulse radiolysis or flash photolysis of nitrite solutions, for which different estimates of the rate constants varied over an order of magnitude. Although selection of the "recommended" values in themselves appears quite reasonable, it is unclear whether the combination of rate constants determined by different methods will result in the correct value of $K_4^2k_5$. The quantity $K_4^2k_5$ determined from the individual rate constants of Schwartz and White is 2.4×10^{-6} M^{-1} s^{-1}, which is a factor of 2.5 larger than the value of 9.4×10^{-7} M^{-1} s^{-1} inferred from the data of Abel and Schmidt[10] assuming a Henry's constant for NO of 1.9×10^{-3} M atm^{-1}.[15] Thus, it is unclear which rate constants should be selected when attempting to accurately model formation of NO and NO_2 from nitrous acid decomposition.

Three studies relating to nitrous acid decomposition have been published since the review of Schwartz and White, the results of which are summarized in Table 1. There are considerable differences in the reported rate constants; these have a dramatic effect on the predicted rate of NO_x production. In addition, hydrolysis of NO_2 has been recently studied with k_5 determined as 4.8×10^7 M^{-1} s^{-1}.[16] Figure 1 illustrates the discrepancies in the literature rate constants, wherein production of NO from decomposition of a 0.01 M nitrous acid solution has been simulated based on the rate constants of the studies in Table 1.

Discrepancies in the reported results are likely caused by the differences in the methods deployed to study the reaction and the assumptions employed when analyzing the data. Park and

Table 1. Summary of Rate Constants for Nitrous Acid Decomposition

	Park and Lee[17] (22 °C)	Beake and Moodie[18] (25 °C)	Schwarz and White[12] (25 °C)	Ram and Stanbury[19] (25 °C)
k_4 (M^{-1} s^{-1})	13.4	15	5.6	10–25
k_{-4} (M^{-1} s^{-1})	1.60×10^8	9.00×10^7	3.00×10^7	1.75×10^8
K_4	8.38×10^{-8}	1.67×10^{-7}	1.87×10^{-7}	$5.7–14.3 \times 10^{-8}$
k_5 (M^{-1} s^{-1})	8.40×10^7	1.00×10^8	7.00×10^7	5.00×10^7
k_{-5} (M^{-2} s^{-1})	0	0.005	0.0089	0.0122
$K_4^2k_5$ (M^{-1} s^{-1})	5.9×10^{-7} (9.2×10^{-7})[a]	2.8×10^{-6}	2.4×10^{-6}	$0.16–1.0 \times 10^{-6}$

[a]Value in parentheses corrected from 22 to 25 °C using the activation energy calculated in the present work.

Lee[17] studied reactions 4 and 5 by employing a chemiluminescence NO_x analyzer to measure the gaseous concentrations of NO, NO_2, and HNO_2 sparged from a solution of nitrous acid. That study assumed that the concentrations of NO and NO_2 were in steady state and that the mass transfer characteristics of NO and NO_2 were the same (and equal to those of CO_2). The rate constant (i.e., $K_4^2k_5$) derived from this study is four times smaller than the recommended values provided by Schwartz and White. A small portion of this difference could be attributed to the slightly lower temperature of the experiments in that study (22 versus 25 °C).

Ram and Stanbury[19] examined reactions of the $IrCl_6^{2-/3-}$ redox couple in nitrous acid over a variety of nitrous acid, nitrate, and hydrogen ion concentrations under conditions where the overall reaction rate was dependent on the rate of reactions 4 and 5. The results of that study depended on the values employed for rate constants of parallel reactions pathways; hence, any errors in the rate constants assumed for parallel reaction pathways in simulations would result in errors in the rate constants for reactions 4 and 5. The resulting values of k_4 ranged from 10 to 25 M^{-1} s^{-1} depending on the experimental conditions, leading to $K_4^2k_5$ values ranging from 1.6×10^{-7} to 1×10^{-6} M^{-1} s^{-1}.

Beake and Moodie[18] studied the decomposition of HNO_2 by UV spectrophotometry at 385 nm in solutions saturated with atmospheric oxygen. The presence of oxygen results in oxidation of NO to NO_2 via reaction 10, which influences the reaction kinetics by reducing the NO concentration, hence driving reaction 4 to the right.

$$2NO + O_2 \rightarrow 2NO_2,\ k_{10} \quad (10)$$

The approach taken was to assume values of the rate constants k_4, k_5, and k_{10} from the literature and to determine the value of k_{-4} by solving the set of ordinary differential equations describing the reaction mechanism and varying k_{-4} to provide the best fit to their experimental data. The results provide a value of $K_4^2k_5$ similar to that of Schwartz and White and considerably larger than that of Park and Lee. An important distinction, as outlined by Butler and Ridd,[6] should be made regarding the rate-limiting reaction step in gas–liquid systems versus purely liquid-phase experiments. In gas–liquid experiments, rapid removal of reaction products can result in rate-limiting formation of N_2O_3 (reaction 6), while in purely aqueous systems reaction 4 rapidly reaches equilibrium and dissolution of NO_2 via reaction 5 becomes the rate-limiting step. Thus, while Beake and Moodie[18] claim to be determining k_{-4}, the result would actually depend on the initially chosen values for k_4 and k_5.

dx.doi.org/10.1021/ic202081z | Inorg. Chem. 2012, 51, 2178–2185

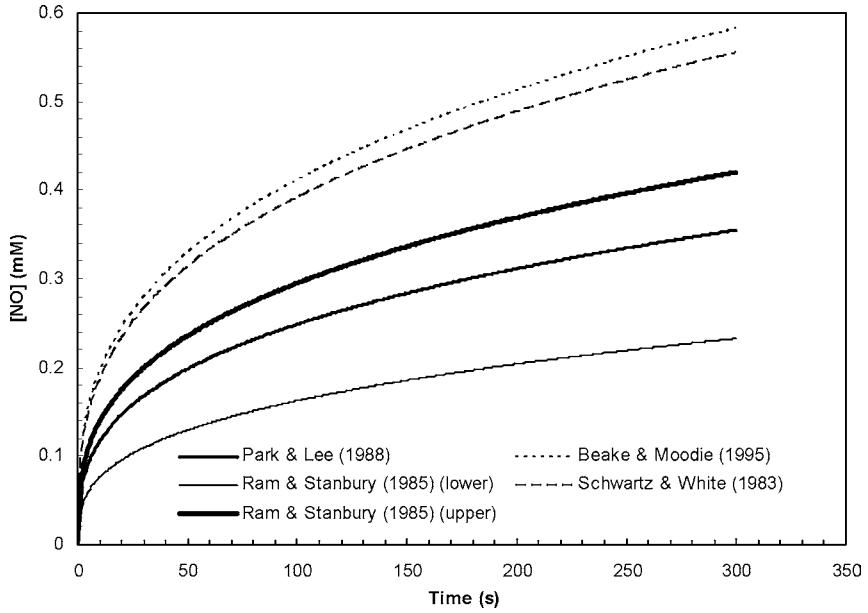

Figure 1. Formation of nitric oxide predicted using literature rate constants for HNO_2 decomposition.

Owing to the discrepancies between reported values for rate constants for nitrous acid decomposition, it is desirable to study the reaction kinetics without the complications of (i) mass transfer between the aqueous and gas phase and (ii) the presence of parallel reaction pathways that influence the reaction kinetics. This can be established by monitoring the decomposition of nitrous acid spectrophotometrically, with precautions taken to prevent any transfer of gases into or out of the reacting solution. Such conditions can be readily achieved in a stopped flow mixing device, wherein two reactant solutions contained in gastight syringes are mixed together rapidly before flowing to a UV−vis observation cuvette. Such a study may yield an accurate value for the quantity $K_4^2k_5$ suitable for modeling NO formation from nitrous acid decomposition during nitrosation reactions.

EXPERIMENTAL SECTION

Decomposition of nitrous acid was studied at concentrations ranging from 2.5 to 100 mM using UV−vis stopped flow spectrophotometry. The setup comprised an Applied Photophysics RX-2000 rapid mixing accessory coupled to a Varian Cary50 spectrophotometer. The temperature of the stopped flow cell was regulated via a Varian Cary peltier thermostatted cell holder, while the drive syringes of the rapid mixing accessory were surrounded by water connected to a circulating cooling/heating bath at the desired reaction temperature. Nitrous acid was generated in situ by reacting a solution of sodium nitrite with a solution of perchloric acid, with an excess of perchloric acid of at least 0.02 M, providing near complete conversion of nitrite ions into nitrous acid. The precise fraction of nitrite converted to nitrous acid was determined by examining the absorbance at 371 and 386 nm as outlined in the Supporting Information.

The ionic strength ranged from 0.08 to 0.2 M, with increasing concentrations of $NaNO_2$ necessitating higher $HClO_4$ concentrations for complete protonation of NO_2^-. Small changes in the ionic strength do not affect the reaction rate because the rate depends only on the concentration of neutral species, whose activity changes minimally with increasing ionic strength. Prior to each kinetic experiment, oxygen was removed from the solutions by sparging them with high-purity nitrogen for at least 20 min. Degassing for longer time periods produced identical results. Reaction kinetics were determined based on the decrease in absorbance at 357.5, 371, and 386 nm. The absorbance at 500 nm (where neither NO or HNO_2 absorbs) was monitored in each experiment to confirm that gas bubbles of nitric oxide were not forming in the solution. Had gas bubbles formed, an increase in absorbance at 500 nm would be observed due to light scattering. The 10 mm path length of the RX-2000 dual path cell was employed for concentrations of 20 mM and below and the 2 mm length utilized for higher concentrations. The total concentration of nitrous acid ($[NO_2^-] + [HNO_2]$) was determined using eq 11, where A is the absorbance at a particular wavelength

$$[HNO_2]_{Total} = [HNO_2]_{Total,initial}\frac{A}{A_{initial}} \quad (11)$$

Equation 11 is valid provided that the ratio of the nitrous acid to nitrite ion concentration remains constant. Employing an excess of hydrogen ions in the experiments ensures that this criteria is met. The reaction kinetics were analyzed by fitting the data from individual experiments over the first 1200 s of reaction to the integrated form of eq 2, which is provided in the Supporting Information. The fitting procedure was performed by employing the solver function in Microsoft Excel to find the value of $K_4^2k_5$ that produced the minimum error between the experimental data and that predicted from the integrated rate equation. In the case of the experiments involving dissolved oxygen at low HNO_2 concentrations, a system of ordinary differential equations describing the reaction mechanism was solved in Polymath 5.1 for different values of $K_4^2k_5$.

Quantum chemistry calculations were performed with the Gaussian 03 software package[20] to investigate the thermochemistry of nitrous acid decomposition. G3B3[21] and CBS-QB3[22] methods were employed for accurate determination of gas-phase reaction free energies, while enthalpies and free energies of solvation were determined at the B3LYP/6-31G(d,p) level[23] with the PCM model (UAHF radii).[24] This was established by comparing the PCM energies to those calculated for the gas phase with the same method and basis sets. Combination of the calculated solvation free energies with the gas-phase free energy of reaction by means of the thermochemical cycle depicted in Figure 2 enabled calculation of the aqueous-phase reaction free energies.

Thermochemical parameters calculated in Gaussian are based on a standard state pressure of 1 atm, while aqueous free energies of reaction employ the 1 M standard state. Results for reaction free energies must therefore be corrected for the change in entropy associated with the transition from a pressure of 1 atm to a concentration of 1 M. This correction has been discussed by Bryantsev et al.[25] and acts to make the free energy of each species 7.9 kJ/mol more positive. Thus, there is no net correction for reactions where there is no change in the number of moles in a reaction, while reactions exhibiting a greater number of

dx.doi.org/10.1021/ic202081z | Inorg. Chem. 2012, 51, 2178−2185

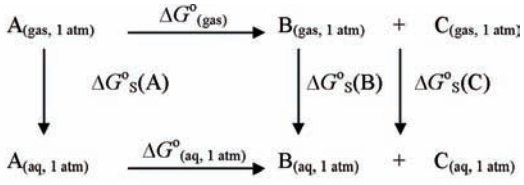

$$\Delta G^{\circ}_{(aq,\,1\ atm)} = \Delta G^{\circ}_{(gas)} + \Delta G^{\circ}_{S}(B) + \Delta G^{\circ}_{S}(C) - \Delta G^{\circ}_{S}(A).$$

$$\Delta G^{\circ}_{(aq,\,1\ M)} = \Delta G^{\circ}_{(aq,\,1\ atm)} + \Delta nRT\ln(24.46)$$

Figure 2. Thermochemical cycle for determining aqueous free energy change of reaction for reaction A → B + C. The value 24.46 reflects the ratio of the molar volume of a gas at 1 atm to that at 1 M.

moles of products than reactants become less favorable in the 1 M standard state and vice versa.

RESULTS AND DISCUSSION

1. Kinetics at 25 °C in Anaerobic Solution. Over the concentration range of interest, reaction 4 is sufficiently rapid to be at equilibrium and the rate of nitrous acid decomposition is therefore dependent on the rate of hydrolysis of NO_2, leading to the simplified rate law given in eq 2. Equation 2 provided an excellent fit to the data, with the value of $K_4^2k_5$ remaining constant at 1.34 (±0.06) × 10^{-6} M^{-1} s^{-1} for nitrous acid concentrations ranging from 0.02 to 0.1 M nitrous acid, demonstrating the validity of this rate law under the present experimental conditions. The kinetics show an initial period of rapid decomposition, after which accumulation of nitric oxide in solution causes a continued decline in the reaction rate. The importance of completely removing oxygen from the reaction medium cannot be stressed enough, particularly at low nitrous acid concentrations where small amounts of oxygen have a significant impact on the reaction kinetics and cause a deviation from the simplified rate equation. As expected from eq 2, the rate of decomposition increases significantly with increasing nitrous acid concentration. At low concentrations of nitrous acid, the rate of reaction declines such that the fraction of nitrous acid decomposed in the time frame of the experiments becomes quite low, leading to small changes in absorbance. Thus, we place the highest confidence in the results obtained for nitrous acid concentrations of 20 mM or greater. Figure 3 shows kinetic traces for 0.02–0.1 M HNO_2 including the best fit of eq 2 to the data. Complete experimental results are tabulated in Appendix A.

The value of $K_4^2k_5$ presently deduced amounts to approximately one-half that recommended by Schwartz and White[12] and determined by Beake and Moodie.[18] It exceeds the largest value of Ram and Stanbury[19] by 30% and surpasses the value of Park and Lee[17] by a similar margin, after correcting that result from 22 to 25 °C. The difference between the present result and that derived from the values recommended by Schwartz and White[12] most likely stems from the uncertainty in the individual constants k_4, k_{-4}, and k_5 of that study, in particular k_{-4}, for which the upper and lower estimates span an order of magnitude. The study of Beake and Moodie employed a similar method to the present study (UV spectroscopy, but with stoppered cells rather than stopped flow) and recorded a significantly larger rate constant. That study concentrated on relatively low HNO_2 concentrations (2–8 mM) and very long reaction times (>3 h), which could have allowed the measurements to be influenced by a slow rate of oxygen diffusion past the cell stopper. In contrast to the measurements of Beake and Moodie, the present result coincides relatively closely with the values of $K_4^2k_5$ deduced from the measurements of Park and Lee and Ram and Stanbury, supporting the present determination.

2. Kinetics at 25 °C in the Presence of Oxygen. To extend our measurements to lower concentrations of nitrous acid (2.5 mM), experiments were performed with solutions initially saturated with atmospheric oxygen. This had the advantages of both increasing the change in absorbance and removing the error associated with the presence of a small amount of residual oxygen in the degassed solutions, which can have a significant effect on the kinetics at low concentrations of nitrous acid. It does, however, introduce some uncertainty owing to the fact that oxidation of NO by O_2 could become at least partially rate limiting, and hence, the

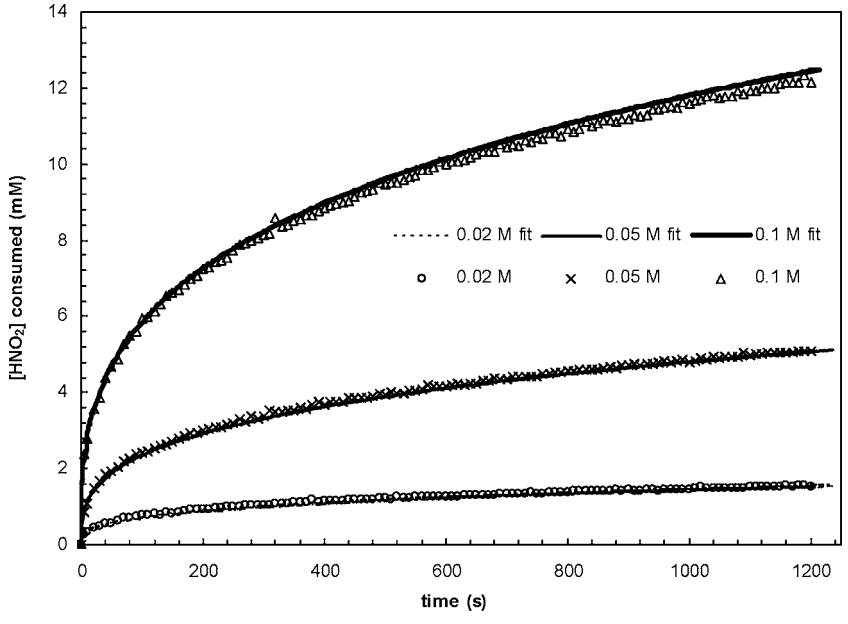

Figure 3. Experimental and simulated nitrous acid decomposition results for 20–100 mM $NaNO_2$. For simulations, $K_4^2k_5$ remains constant at 1.34 × 10^{-6} M^{-1} s^{-1}.

dx.doi.org/10.1021/ic202081z | Inorg. Chem. 2012, 51, 2178–2185

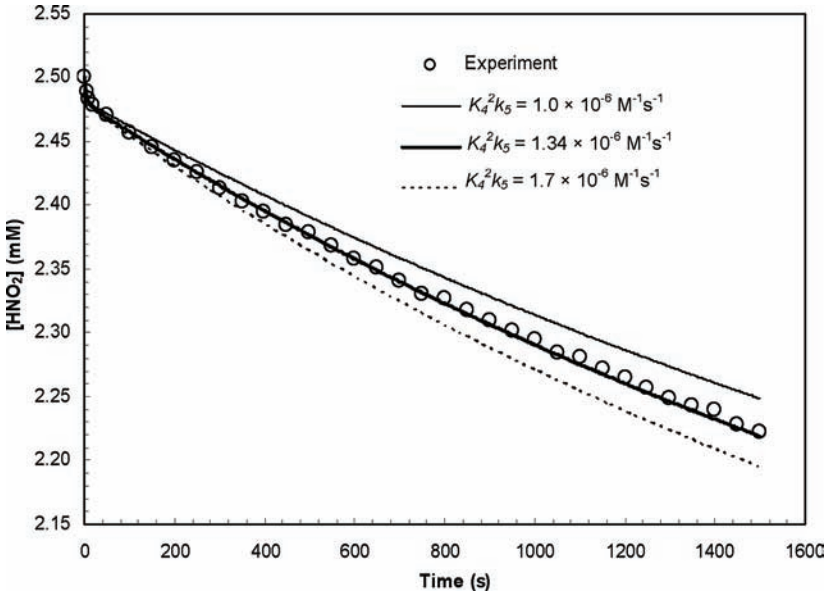

Figure 4. Comparison of experimental result and simulations for decomposition of 2.5 mM HNO_2 in air-saturated solutions.

values determined would depend on the rate constant assumed for that reaction. Oxidation of NO to NO_2 by O_2 is a third-order reaction, second order in NO and first order in O_2[26] (reaction 10). Rate constants for that reaction have been determined in a number of studies with estimates ranging from 1.6 to 2.9 × 10^6 M^{-2} s^{-1}.[27] A value of k_{10} =2.1 × 10^6 M^{-2} s^{-1}, consistent with the results of Lewis and Dean,[26] provides an identical value of $K_4^2k_5$ to that in the anaerobic experiments. Figure 4 compares the results for decomposition of 2.5 mM HNO_2 in air-saturated solutions to simulations for different values of $K_4^2k_5$.

3. Kinetics of the Reverse Reaction. Under the conditions of the present study with relatively low nitrite and acid concentrations, nitrate ions are produced at sufficiently low concentrations that hydrolysis of NO_2 (reaction 5) can be assumed to be irreversible. In the presence of added nitrate or very high acid concentrations the reverse of reaction 5 results in formation of NO_2, reducing the net rate of nitrous acid decomposition. This reaction exhibits first-order dependencies on nitrous acid, hydrogen ion, and nitrate ion concentrations.[28,29] Analogous rate laws are observed for the nitrosation of a range of species by nitrous acid,[4] suggesting that a similar mechanism operates for the reaction of nitrous acid and nitrate. The rate law for nitrous acid decomposition can be modified to incorporate the effect of this reaction by assuming that the rate of decomposition depends on the net rate of NO_2 hydrolysis, i.e., the net rate of reaction 5a.

$$2NO_2 + H_2O \leftrightarrows HNO_2 + NO_3^- + H^+,\ k_5,\ k_{-5} \quad (5a)$$

$$\frac{d[HNO_2]}{dt} = -\frac{3K_4^2k_5[HNO_2]^4}{[NO]^2} + 3k_{-5}[HNO_2][H^+][NO_3^-] \quad (12)$$

Experiments with added nitrate ions showed a similar initial rate of decomposition but did not proceed to as great an extent as the accumulation of NO eventually makes the two terms of eq 12 equal, that is, the presence of nitrate causes the reactions to reach an equilibrium position. Figure 5 provides a comparison of a kinetic trace for 0.1 M NO_3^- to an equivalent experiment with no added nitrate. The constant k_{-5} was evaluated by performing a series of experiments with different hydrogen and nitrate ion concentrations and ascertained to be 5.9 (±0.6) × 10^{-3} M^{-2} s^{-1} at an ionic strength of 0.18 M. This result is 20−40% smaller compared to previous values reported in the literature at zero ionic strength.[12] This discrepancy arises as a result of nonunity activity coefficients of nitrate and hydrogen ions at 0.18 M ionic strength, which reduce the observed rate of the reverse reaction. Our result lies in close agreement with the prior determination by Abel and Schmidt[30] and Jordan and Bonner.[28] This provides further support for the value of $K_4^2k_5$ (1.34 × 10^{-6} M^{-1} s^{-1}) determined in the present study as employing this constant in eq 12 results in the same value of k_{-5} determined independently in the literature. Had the value of $K_4^2k_5$ been in error, it would not have been possible to reproduce the correct value of k_{-5}.

4. Temperature Dependence and Thermochemical Analysis of the Elementary Reaction Mechanism. The temperature dependence of both the forward and the reverse reactions was examined between 20 and 55 °C. The rate of nitrous acid decomposition increased markedly with increasing temperature, a plot of $\ln(K_4^2k_5)$ yielding an apparent activation energy of 106.6 ± 3 kJ mol^{-1}. The uncertainty represents the standard error obtained from a plot of $\ln(K_4^2k_5)$ versus $1/T$, which was determined using the linest function in Microsoft Excel. This large activation energy may have contributed to the considerable scatter in the literature data, with a temperature increase of just 1 °C resulting in an increase in $K_4^2k_5$ of approximately 20% at 25 °C. This underscores the importance of accurately maintaining a constant temperature when studying this reaction. The activation energy of the reverse reaction was determined to be 76 ± 4 kJ mol^{-1}, in close agreement with the prior determination of 74 kJ mol^{-1} by Akhtar et al.[29]

A quantum chemistry study was undertaken to determine the origin of the high activation energy associated with $K_4^2k_5$. The gas-phase free energies and enthalpies of reactions 6−9 were established using the average results of the CBS-QB3 and G3B3 methods. The gas-phase free energy of the proton, −26.3 kJ/mol, was taken from the literature.[31] Nitrous acid exists in both the cis and the trans conformations, with the energy of the cis isomer

dx.doi.org/10.1021/ic202081z | Inorg. Chem. 2012, 51, 2178−2185

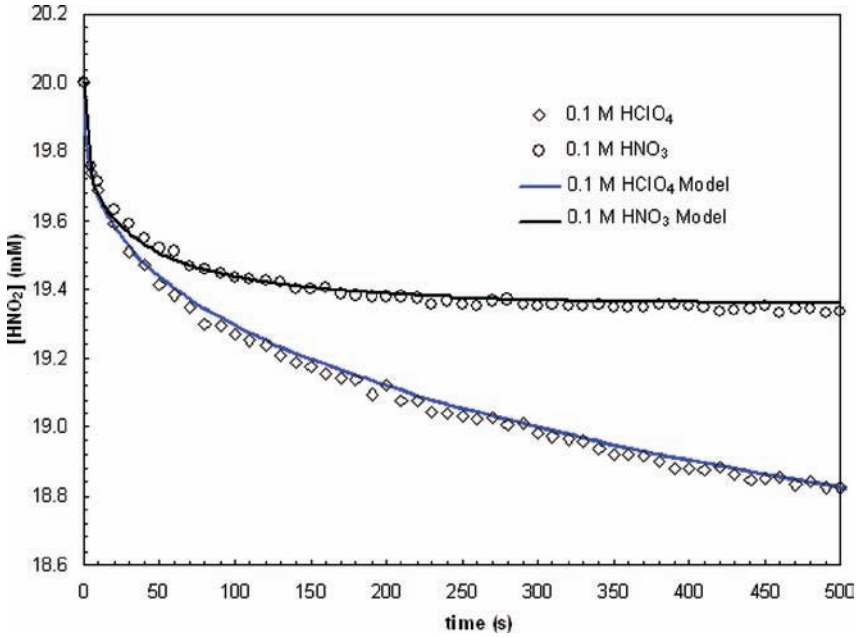

Figure 5. Experiment and model for decomposition of 0.02 M HNO_2 in 0.1 M $HClO_4$ and 0.1 M HNO_3.

Table 2. Calculated Aqueous Enthalpies and Free Energies of Reactions 6−9 and Comparison of Calculated and Experimental Equilibrium Constants (all energies are in kJ)

reaction	ΔH_{298}G3B3	ΔH_{298}CBS-QB3	ΔG_{298}G3B3	ΔG_{298}CBS-QB3	K_{calcd} [a]	K_{expt}	unit	ref
6	−4.0	−2.4	25.2	27.0	2.65×10^{-5}	3×10^{-3}	M^{-1}	37
7	50.7	46.9	15.4	11.6	4.30×10^{-3}	3.3×10^{-5}	M	12
8	−69.3	−66.6	−19.4	−16.5	1.39×10^{3}	7×10^{4}	M^{-1}	12
9	−18.5	−26.9	−24.3	−32.9	1.04×10^{5}	1.25×10^{5}	M	12
4 (6 + 7)	46.7	44.5	40.7	38.6	1.14×10^{-7}	1.87×10^{-7}		12

[a] Calculated equilibrium constants are based on the average of G3B3 and CBS-QB3 results.

located 2.2 and 2.5 kJ higher than trans for CBS-QB3 and G3B3, respectively. Owing to the small difference in the calculated energy of HONO isomers, we use the average energy when determining all thermodynamic quantities, as previously reported.[32] The first reaction results in formation of dinitrogen trioxide and involves the combination of two nitrous acid molecules with simultaneous elimination of H_2O (reaction 6). The transition states (TS) for the gas-phase reaction have previously been identified,[33,34] and because this reaction has been demonstrated to be at equilibrium,[9] we did not investigate the TS further. N_2O_3 undergoes homolytic fission producing NO and NO_2, followed by combination of two NO_2 molecules forming N_2O_4. The final reaction involves hydrolysis of N_2O_4, forming nitrous acid, nitrate, and hydrogen ions. The calculated gas-phase enthalpies and free energies of reaction are in good agreement with experimental values,[35] with mean absolute errors in the gas-phase ΔH_r and ΔG_r of 1.9 kJ and 3.0 kJ/mol respectively, for reactions 6−8. There was however a significant difference of 14 kJ/mol between the experimental results for reaction 9 and those calculated with the CBS-QB3 method, inclusion of which increases the average error in ΔH_r to 3.5 kJ/mol.

The aqueous-phase enthalpies and free energies of reaction were determined by combining the solvation enthalpies and free energies determined with the PCM solvent model to the accurate gas-phase results in accordance with the thermochemical cycle depicted in Figure 2. In the case of water and the hydrogen cation, the experimental enthalpies and free energies of vaporization were applied, as opposed to the calculated ones.[35,36] Table 2 presents the calculated aqueous enthalpies and free energies of reaction for reactions 6−9, including the calculated equilibrium constants which are compared to experimental results. Note that the free energies include a correction for a change in standard state from 1 atm to 1 M[25] and that the calculated equilibrium constants are derived based on the average of G3B3 and CBS-QB3 free energies of reaction.

Table 2 shows that the predicted equilibrium constants for reactions 6 and 7 deviate from the experimental values by 2 orders of magnitude, equivalent to a 12 kJ error in ΔG_r. The predicted equilibrium constant for reaction 8 is almost 2 orders of magnitude smaller than the experimental value. The higher error of the aqueous reaction free energies relative to the gas-phase results arises due to inaccuracies in the prediction of solvation free energies, which are typically in the order of 4 kJ/mol for neutral species.[38] With regard to reactions 7 and 8, the present method predicts that formation of the compound oxides N_2O_3 and N_2O_4 (from the simple oxides NO and NO_2) is considerably less favorable than predicted from experiments. Considering that the calculated gas-phase energies are in good agreement with experimental results, it appears that the PCM model underestimates the solvation free energies of N_2O_4 and N_2O_3 relative to the simple oxides NO and NO_2. Despite the errors associated with K_6 and K_7, combining reactions 6 and 7 into the overall reaction 4 provides close agreement between the calculated and the experimental equilibrium constants. The results for reaction 9 with CBS-QB3 and G3B3 differ by 8.6 kJ/mol; however, the average is fortuitously in excellent agreement with experiments.

dx.doi.org/10.1021/ic202081z | Inorg. Chem. 2012, 51, 2178−2185

The calculated enthalpy of reaction 4 can be employed to determine the contribution of this reaction to the activation energy of $K_4^2k_5$ by means of eq 13. Provided that the enthalpy of reaction is independent of temperature, a plot of $\ln(K)$ versus the reciprocal of temperature is linear with a slope equal to the negative of the enthalpy of reaction. Combining the expression for the equilibrium constant with the Arrhenius expression for the temperature dependence of reaction 5 yields 5 yields eq 13, as shown in the Supporting Information. Thus, the apparent activation energy, determined from of a plot of $\ln(K_4^2k_5)$ versus $1/T$, is equal to twice the enthalpy of reaction 4 summed with the activation energy of reaction 5.

$$\ln(K_4^2k_5) = -\frac{(2\Delta H_{(4)} + E_{A(5)})}{RT} + 2\frac{\Delta S_{(4)}}{R} + \ln(A) \quad (13)$$

Reaction 4 is considerably endothermic, with gas-phase enthalpies of reaction of 34.4 and 37.7 kJ at the G3B3 and CBS-QB3 levels, respectively. The effect of solvation serves to make the reaction more endothermic, leading to an average value of 45 kJ for the aqueous enthalpy of reaction 4. Thus, this reaction contributes approximately 90 kJ to the apparent activation energy of $K_4^2k_5$ due to the second-order dependence on K_4. It can therefore be concluded that reaction 5 has a small activation energy on the order of 17 kJ. Although the solvation energies introduce some uncertainty in the value of $\Delta H_{(4)}$, the contribution of K_4^2 to the apparent activation energy is clearly much higher than the contribution of k_5. The close agreement between the experimental and the calculated free energies for reaction 4 gives us confidence in the calculated enthalpy of reaction.

CONCLUSION

Decomposition of nitrous acid including the reverse reaction between nitrous acid and nitrate ions has been studied by stopped flow spectrophotometry to resolve discrepancies in literature values of the rate constants. The value determined ($K_4^2k_5 = 1.34 \pm (0.06) \times 10^{-6}$ M^{-1} s^{-1}) is of higher accuracy than those previously reported in the literature as it does not depend on the rate of parallel reaction pathways or on the rate of interphase mass transfer of gaseous reaction products. The activation energy associated with $K_4^2k_5$ is 107 kJ, the majority of this being attributable to the endothermic nature of the reaction $2HONO \leftrightarrows NO + NO_2 + H_2O$.

APPENDIX A: EXPERIMENTAL DATA FOR NITROUS ACID DECOMPOSITION

Table A1. Rate Constants at 298 K for HNO_2 Decomposition

experiment	$NaNO_2$ (M)	$HClO_4$ (M)	$NaClO_4$ (M)	T (K)	$K_4^2k_5$ (M^{-1} s^{-1})
1	0.02	0.04	0.04	298.15	1.39×10^{-6}
2	0.02	0.1	0.08	298.15	1.37×10^{-6}
3	0.02	0.1	0.08	298.15	1.33×10^{-6}
4	0.02	0.1	0.08	298.15	1.35×10^{-6}
5	0.05	0.1	0.05	298.15	1.33×10^{-6}
6	0.05	0.1	0.05	298.15	1.29×10^{-6}
7	0.05	0.1	0.05	298.15	1.34×10^{-6}
8	0.05	0.1	0.05	298.15	1.32×10^{-6}
9	0.1	0.15	0.05	298.15	1.46×10^{-6}
10	0.1	0.15	0.05	298.15	1.32×10^{-6}
11	0.1	0.15	0.05	298.15	1.21×10^{-6}

Table A2. Temperature Dependence of Nitrous Acid Decomposition

experiment	$NaNO_2$ (M)	$HClO_4$ (M)	$NaClO_4$ (M)	T (K)	$K_4^2k_5$ (M^{-1} s^{-1})
12	0.02	0.04	0.04	308.15	5.77×10^{-6}
13	0.02	0.04	0.04	293.15	6.82×10^{-7}
14	0.02	0.04	0.04	293.15	6.82×10^{-7}
15	0.02	0.04	0.04	303.55	3.44×10^{-6}
16	0.02	0.04	0.04	313.35	1.16×10^{-5}
17	0.02	0.04	0.04	287.75	2.73×10^{-7}
18	0.02	0.04	0.04	288.15	4.22×10^{-7}
19	0.02	0.1	0.08	308.15	6.51×10^{-6}
20	0.02	0.04	0.04	288.15	2.35×10^{-7}

Table A3. Rate Constants for Reverse Reaction at 298 K

experiment	H^+ (M)	NO_3^- (M)	$NaNO_2$ (M)	k_{-5} (M^{-2} s^{-1})
21	0.05	0.05	0.02	6.48×10^{-3}
22	0.05	0.05	0.02	6.69×10^{-3}
23	0.1	0.05	0.02	6.23×10^{-3}
24	0.1	0.05	0.02	5.13×10^{-3}
25	0.1	0.15	0.02	5.33×10^{-3}
26	0.1	0.15	0.02	5.87×10^{-3}
27	0.1	0.1	0.02	5.28×10^{-3}
28	0.1	0.1	0.02	5.83×10^{-3}

Table A4. Temperature Dependence of Reverse Reaction Determined in 0.02 M $NaNO_2$, 0.1 M H^+, and 0.1 M NO_3^-

experiment	T (K)	k_{-5} (M^{-2} s^{-1})
29	308	1.44×10^{-2}
30	308	1.18×10^{-2}
31	318	3.91×10^{-2}
32	318	4.59×10^{-2}
33	328	9.45×10^{-2}
34	328	1.06×10^{-1}

ASSOCIATED CONTENT

Supporting Information

Derivation of selected equations, calculated geometries, frequencies, moments of inertia, enthalpies, free energies, solvation free energies, and solvation enthalpies. This material is available free of charge via the Internet at http://pubs.acs.org.

AUTHOR INFORMATION

Corresponding Author

*Phone: +61 2 4985-4433. Fax: +61 2 4921-6893. E-mail: Bogdan.Dlugogorski@newcastle.edu.au.

ACKNOWLEDGMENTS

Financial support from Dyno Nobel Asia Pacific Pty. Ltd. and the Australian Research Council is gratefully acknowledged.

REFERENCES

(1) Patwardhan, J.; Joshi, J. *AIChE J.* **2003**, *49*, 2728–2748.
(2) Ingale, N. D.; Chatterjee, I. B.; Joshi, J. B. *Chem. Eng. J. (Amsterdam, Neth.)* **2009**, *155*, 851–858.
(3) Zollinger, H. *Azo and diazo chemistry: Aliphatic and Aromatic Compounds*; Interscience Publishers Inc.: New York, 1961.
(4) Williams, D. L. H. *Nitrosation Reactions and the Chemistry of Nitric Oxide*; Elsevier B. V.: Amsterdam, 2004.

(5) Finlayson-Pitts, B. J.; Pitts, J. N. J. *Atmospheric Chemistry: Fundamentals and Experimental Techniques*; Wiley: New York, 1986.
(6) Butler, A. R.; Ridd, J. H. *Nitric Oxide* **2004**, *10*, 20−24.
(7) Aga, R. G.; Hughes, M. N. *Methods Enzymol.* **2008**, *436*, 35−48.
(8) Klepper, L. *Plant Phsiol.* **1990**, *93*, 26−32.
(9) da Silva, G.; Dlugogorski, B. Z.; Kennedy, E. M. *Chem. Eng. Sci.* **2006**, *61*, 3186−3197.
(10) Abel, E.; Schmid, H. *Z. Phys. Chem.* **1928**, *134*, 279−300.
(11) da Silva, G. R.; Dlugogorski, B. Z.; Kennedy, E. M. *Int. J. Chem. Kinet.* **2007**, *39*, 645−656.
(12) Schwartz, S. E.; White, W. H. *Adv. Environ. Sci. Technol.* **1983**, *12*, 1−116.
(13) Bunton, C. A.; Llewellyn, D. R.; Stedman, G. *J. Chem. Soc.* **1959**, 568−573.
(14) Hughes, E. E.; Ridd, J. H. *J. Chem. Soc.* **1958**, 70−76.
(15) Armor, J. N. *J. Chem. Eng. Data* **1974**, *19*, 82−84.
(16) Becker, R. H.; Nicoson, J. S.; Margerum, D. W. *Inorg. Chem.* **2003**, *42*, 7938−7944.
(17) Park, J. Y.; Lee, Y. N. *J. Phys. Chem.* **1988**, *92*, 6294−302.
(18) Beake, B. D.; Moodie, R. B. *J. Chem. Soc., Perkin Trans. 2* **1995**, 1045−8.
(19) Ram, M. S.; Stanbury, D. M. *Inorg. Chem.* **1985**, *24*, 2954−62.
(20) Frisch, M. J.; Trucks, G. W.; Schlegel, H. B.; Scuseria, G. E.; Robb, M. A.; Cheeseman, J. R.; Montgomery, J. A., Jr.; Vreven, T.; Kudin, K. N.; Burant, J. C.; Millam, J. M.; Iyengar, S. S.; Tomasi, J.; Barone, V.; Mennucci, B.; Cossi, M.; Scalmani, G.; Rega, N.; Petersson, G. A.; Nakatsuji, H.; Hada, M.; Ehara, M.; Toyota, K.; Fukuda, R.; Hasegawa, J.; Ishida, M.; Nakajima, T.; Honda, Y.; Kitao, O.; Nakai, H.; Klene, M.; Li, X., Knox, J. E; Hratchian, H. P.; Cross, J. B.; Bakken, V.; Adamo, C.; Jaramillo, J.; Gomperts, R.; Stratmann, R. E.; Yazyev, O.; Austin, A. J.; Cammi, R.; Pomelli, C.; Ochterski, J. W.; Ayala, P. Y.; Morokuma, K.; Voth, G. A.; Salvador, P.; Dannenberg, J. J.; Zakrzewski, V. G.; Dapprich, S.; Daniels, A. D.; Strain, M. C.; Farkas, O.; Malick, D. K.; Rabuck, A. D.; Raghavachari, K.; Foresman, J. B.; Ortiz, J. V.; Cui, Q.; Baboul, A. G.; Clifford, S.; Cioslowski, J.; Stefanov, B. B.; Liu, G.; Liashenko, A.; Piskorz, P.; Komaromi, I.; Martin, R. L.; Fox, D. J.; Keith, T.; Al-Laham, M. A.; Peng, C. Y.; Nanayakkara, A.; Challacombe, M.; Gill, P. M. W.; Johnson, B.; Chen, W.; Wong, M. W.; Gonzalez, C.; Pople, J. A. *Gaussian 03*, Revision B.05; Gaussian Inc.: Pittsburgh, PA, 2003.
(21) Baboul, A. G.; Curtiss, L. A.; Redfern, P. C.; Raghavachari, K. *J. Chem. Phys.* **1999**, *110*, 7650−7657.
(22) Montgomery, J. A.; Ochterski, J. W.; Petersson, G. A. *J. Chem. Phys.* **1994**, *101*, 5900−5909.
(23) Becke, A. D. *J. Chem. Phys.* **1993**, *98*, 5648−5652.
(24) Tomasi, J.; Mennucci, B.; Cances, E. *J. Mol. Struct.: THEOCHEM* **1999**, *464*, 211−226.
(25) Bryantsev, V. S.; Diallo, M. S.; Goddard, W. A. III *J. Phys. Chem. B* **2008**, *112*, 9709−9719.
(26) Lewis, R. S.; Deen, W. M. *Chem. Res. Toxicol.* **1994**, *7*, 568−574.
(27) Goldstein, S.; Czapski, G. *J. Am. Chem. Soc.* **1995**, *117*, 12078−12084.
(28) Jordan, S.; Bonner, F. T. *Inorg. Chem.* **1973**, *12*, 1369−1373.
(29) Akhtar, M. J.; Axente, D.; Bonner, F. T. *J. Chem. Phys.* **1979**, *71*, 3570−3572.
(30) Abel, E.; Schmid, H. *Z. Phys. Chem.* **1928**, *136*, 430−6.
(31) Liptak, M. D.; Shields, G. C. *J. Am. Chem. Soc.* **2001**, *123*, 7314−7319.
(32) da Silva, G.; Kennedy, E. M.; Dlugogorski, B. Z. *J. Phys. Chem. A* **2006**, *110*, 11371−11376.
(33) Mebel, A. M.; Lin, M. C.; Melius, C. F. *J. Phys. Chem. A* **1998**, *102*, 1803−1807.
(34) Tantanak, D.; Hillier, I. H.; Vincent, M. A. *J. Mol. Struct.: THEOCHEM* **2003**, *626*, 239−246.
(35) Linstrom, P. J.; Mallard, W. G. *NIST Chemistry WebBook*, NIST Standard Reference Database Number 69. http://webbook.nist.gov (Sept 12, 2011),
(36) Tissandier, M. D.; Cowen, K. A.; Feng, W. Y.; Gundlach, E.; Cohen, M. H.; Earhart, A. D.; Coe, J. V.; Tuttle, T. R. *J. Phys. Chem. A* **1998**, *102*, 7787−7794.
(37) Markovits, G. Y.; Schwartz, S. E.; Newman, L. *Inorg. Chem.* **1981**, *20*, 445−450.
(38) Marenich, A. V.; Cramer, C. J.; Truhlar, D. G. *J. Phys. Chem. B* **2009**, *113*, 6378−6396.